International Journal of Robust and Nonlinear Control

WILEY

RESEARCH ARTICLE OPEN ACCESS

Homogeneous Observer-Based Affine Formation Tracking

Rodrigo Aldana-López[1,2] | Miguel Aranda[3] | Rosario Aragüés[3] | Carlos Sagüés[3]

[1]Intel Labs, Intel Tecnología de México, Zapopan, Mexico | [2]Unidad Guadalajara, Cinvestav, Zapopan, Jalisco, Mexico | [3]Departamento de Informática e Ingeniería de Sistemas (DIIS) and Instituto de Investigación en Ingeniería de Aragón (I3A), Universidad de Zaragoza, Zaragoza, Spain

Correspondence: Rodrigo Aldana-López (rodrigo.aldana.lopez@gmail.com)

Received: 6 February 2025 | **Revised:** 22 September 2025 | **Accepted:** 5 November 2025

Funding: This work was supported by Gobierno de Aragón under Project DGA T45-23R, project REMAIN S1/1.1/E0111 (Interreg Sudoe Programme, ERDF), projects PID2021-124137OB-I00, and PID2024-159279OB-I00 funded by MCIN/AEI/10.13039/501100011033, by ERDF A way of making Europe and by the European Union NextGenerationEU/PRTR, Consejo Nacional de Ciencia y Tecnología (CONACYT-Mexico) with grant number 739841, and Universidad de Zaragoza and Banco Santander.

Keywords: distributed estimation | multi-agent formation control | sliding mode algorithms

ABSTRACT

This article addresses the control of mobile agents, termed followers, to track a time-varying affine formation specified by a set of leaders. We present a distributed hierarchical method composed of a homogeneous high-order sliding mode observer and a tracking controller. The observer estimates the followers' target trajectories from neighbor information in finite time and is robust to measurement noise. Compared to existing approaches, the method accommodates heterogeneous follower dynamics, maintains estimation accuracy independently of follower motion, and mitigates chattering effects. Convergence is guaranteed for both continuous- and discrete-time implementations, which are supported by formal analysis and numerical simulations.

1 | Introduction

In multi-agent systems, formation control is a central problem concerned with achieving and maintaining specific geometric arrangements among agents [1]. Such formations, often defined through graph specifications, are critical for applications ranging from collective sensing [2] and cooperative navigation [3] to tasks such as collaborative object transport [4]. Over the years, a wide range of approaches to formation control have been developed. In particular, distance-based [5] and position-based [6] strategies have been popular in the literature. Bearing-based methods have also emerged [3], where formations are stabilized through relative bearing information instead of positions or distances. Another active line has focused on strategies built on complex Laplacian formulations [7, 8], which can be applied to formation control and distributed localization in dynamic networks.

Affine formations constitute a particular class where the achieved configuration is an affine transformation of a nominal pattern [9–17]. This means that agent positions evolve through combinations of translation, rotation, scaling, and shearing applied to the nominal configuration. Compared to translation-based formations [6, 18–20] or rigid formations [5, 21], affine formations enable richer maneuvering capabilities, which is especially valuable when teams must adapt to environmental constraints such as traversing narrow passages. Another appealing feature is that affine formations can be controlled through distributed algorithms with a linear core structure. In this setting, the stress matrix [10] plays a role analogous to the Laplacian in consensus-based formation control [6, 20], serving as the key structure for analysis and design.

A number of studies have advanced affine formation control from different perspectives. The affine formation maneuvering problem was introduced in [10], showing that leader trajectories define the target configuration and that followers can be controlled accordingly. A scheme was later considered in [11] where one special leader computes the time-varying affine parameters,

and the other leaders estimate them through a sliding-mode observer; moreover, the control design for the followers assumes that they have high-order dynamics. A distributed sliding-mode estimator was designed in [12], inspired by [6], so that followers can estimate their own target positions in the formation. Restrictions to planar affine formations consisting only of translation, rotation, and uniform scaling were analyzed in [13], where leaders estimate parameters locally through direct measurements and without communications. The framework was extended in [22] to directed graphs, higher-order agent dynamics, and time delays. A two-layer control strategy for leaders and followers under Euler–Lagrange dynamics that ensures practical finite-time convergence was presented in [14]. Building on the leaderless approach of [9], a unified sliding-mode control law applicable to affine, rigid, and translational formations but limited to first-order models was given in [15]. Heterogeneity across agents was studied in [16] by allowing dissimilar parameters while still assuming first-order dynamics. Timed convergence guarantees were addressed in [17] and [23]: the former proposed a prescribed-time convergent controller using a scaling time function, while the latter employed time-base generators to ensure fixed-time convergence, both requiring a shared clock reference across agents. Other works [24, 25] applied optimization frameworks to enhance the performance of affine formation control. The linear formation control formulation presented in [26] extends standard affine formation control by defining nominal configurations in higher dimensions. Taken together, these contributions establish a solid foundation for affine formation control, covering problem formulation, heterogeneity, and convergence guarantees. Yet, most approaches rely on either low-order observers, restrictive agent models, or specific structural assumptions such as synchronized clocks or leader–follower hierarchies.

One way to address some of these issues is through hierarchical observer–controller designs. By separating estimation from control, such schemes allow observers to handle uncertainty, noise, or discrete communication constraints, while controllers focus on motion dynamics. This separation has been successfully exploited in several formation control settings though mostly outside the affine setting. An observer was used in [6] to estimate the state of a virtual leader, while centroid estimation was the focus in [27], and centroid-based strategies were extended to multiple leaders in [20]. Other works have employed observers to estimate statistical moments that describe the formation's shape [28, 29], the target positions and velocities of the agents [30], or the overall state of the formation [31]. These studies highlight the usefulness of hierarchical observer–controller designs, but they are tailored to formations modeled through Laplacian dynamics. Affine formations, by contrast, are governed by stress-matrix dynamics and thus require different analysis tools.

One of the central challenges in affine formation tracking is that leader motions define a persistently time-varying target configuration. Observers must therefore follow trajectories that evolve continuously rather than static references, and controllers must remain effective despite discretization, noise, and modeling imperfections. To cope with this variability, methods with strong robustness and finite-time convergence properties are especially suitable. In this context, sliding-mode techniques have played an important role in the design of both observers and controllers. Classical sliding-mode control approaches have been applied in affine formation tracking. For instance, a first-order sliding mode (FOSM) approach was proposed in [32], with a related hierarchical approach in [33]. While classical sliding-mode observers are attractive due to their finite-time convergence, they are affected by chattering and sensitivity to noise. High-order sliding mode (HOSM) observers [34, 35] overcome these limitations by exploiting weighted homogeneity, which yields finite-time convergence while reducing chattering and improving robustness to discretization and disturbances. HOSM-based algorithms have been applied to distributed consensus problems [20, 36–38], where they enable robust estimation of dynamic averages and their derivatives. However, these works address Laplacian-driven consensus problems, not affine formation tracking.

Motivated by this discussion, we propose a distributed observer–controller scheme for affine formation tracking in multi-agent systems. The scheme consists of a homogeneous HOSM observer and a position tracking controller, and has the following distinctive features:

- The first application of HOSM observers to affine formation tracking.
- A hierarchical observer–controller structure that decouples estimation from control, allowing heterogeneous follower dynamics and flexible motion controller designs.
- A novel adaptation of HOSM to a problem fundamentally different from prior uses (e.g., dynamic average consensus), requiring a distinct design and analysis.
- The first formal analysis of affine formation tracking under both discretization and measurement noise, covering continuous-time and discrete-time implementations.

1.1 | Notation

Let $\mathbb{R}, \mathbb{N}$ be the sets of real and natural numbers respectively. Let $\text{sign}(x) = 1$ if $x > 0$, $\text{sign}(x) = -1$ if $x < 0$ and $\text{sign}(0) = 0$. Moreover, if $x \in \mathbb{R}$, let $\lceil x \rfloor^\alpha := |x|^\alpha \text{sign}(x)$ for $\alpha > 0$ and $\lceil x \rfloor^0 := \text{sign}(x)$. In the vector case $\mathbf{x} = [x_1, \dots, x_n]^\top \in \mathbb{R}^n$, then $\lceil \mathbf{x} \rfloor^\alpha := [\lceil x_1 \rfloor^\alpha, \dots, \lceil x_n \rfloor^\alpha]^\top$ for $\alpha \geq 0$. Let $\sigma_{\min}(\bullet), \sigma_{\max}(\bullet)$ denote the minimum and maximum singular values. For a non-negative integer m, the m-th derivative of a function $f(t)$ is denoted as $f^{(m)}(t)$ with $\dot{f}(t) := f^{(1)}(t)$.

2 | Preliminaries

Consider $N \in \mathbb{N}$ agents, which can move in $\mathbb{R}^d$ with $d \geq 2$ and $N \geq d + 1$, identified for convenience by an index in the set $\mathcal{I} := \{1, \dots, N\}$. Let $N_L < N$ leaders indexed by $\mathcal{I}_L := \{1, \dots, N_L\} \subseteq \mathcal{I}$. Moreover, consider N_F followers such that $N_L + N_F = N$, and denote the set of their indices by $\mathcal{I}_F := \mathcal{I} \setminus \mathcal{I}_L$. In subsequent developments, we use the same symbol $i \in \mathcal{I}$ for an agent index, regardless of whether it is used for a leader or a follower, where the distinction is made by specifying if $i \in \mathcal{I}_L$ or $i \in \mathcal{I}_F$ respectively, or simply $i \in \mathcal{I}$ when no distinction is required.

The interaction between agents is modeled by an undirected graph $\mathcal{G} = (\mathcal{I}, \mathcal{E})$, where the agent index set $\mathcal{I}$ is the corresponding

node set and $\mathcal{E} \subseteq \mathcal{I} \times \mathcal{I}$ is the edge set. Denote with $\mathcal{N}_i$ the set of neighbors of agent $i \in \mathcal{I}$ according to $\mathcal{G}$.

Given an arbitrary agent $i \in \mathcal{I}$, its position at time t is denoted by $\mathbf{p}_i(t) \in \mathbb{R}^d$. A nominal formation is specified by the graph $\mathcal{G}$ together with a constant configuration of nominal positions $\{\mathbf{p}_i^*\}_{i\in\mathcal{I}}$ for all N agents. The goal is not for the agents to reach these nominal positions exactly, but rather a formation obtained from them by an affine transformation, uniquely determined by the leaders' positions. To clarify this, consider the following definitions and results we borrow from [10].

Definition 1. Let the affine image $\mathcal{A}(\mathbf{p}_1^*, \ldots, \mathbf{p}_N^*)$ of the nominal configuration be the set of all stacked agent positions for which, for each one of them, there exist $\mathbf{A} \in \mathbb{R}^{d\times d}$ and $\mathbf{b} \in \mathbb{R}^d$ satisfying $\mathbf{p}_i = \mathbf{A}\mathbf{p}_i^* + \mathbf{b}$ for all i. Formally,

$$\mathcal{A}(\mathbf{p}_1^*, \ldots, \mathbf{p}_N^*) = \big\{\mathbf{p} = [\mathbf{p}_1^\top, \ldots, \mathbf{p}_N^\top]^\top \in \mathbb{R}^{dN} : \exists\, \mathbf{A} \in \mathbb{R}^{d\times d}, \mathbf{b} \in \mathbb{R}^d, \quad \mathbf{p}_i = \mathbf{A}\mathbf{p}_i^* + \mathbf{b}\ \forall i \in \mathcal{I}\big\}.$$

Definition 2. Let the decomposition

$$\mathbf{p} = \begin{bmatrix}\mathbf{p}_L \\ \mathbf{p}_F\end{bmatrix},\ \mathbf{p}_L = \begin{bmatrix}\mathbf{p}_1 \\ \vdots \\ \mathbf{p}_{N_L}\end{bmatrix},\ \mathbf{p}_F = \begin{bmatrix}\mathbf{p}_{N_L+1} \\ \vdots \\ \mathbf{p}_N\end{bmatrix}.$$

The nominal formation is affinely localizable by the leaders if for any $\mathbf{p} \in \mathcal{A}(\mathbf{p}_1^*, \ldots, \mathbf{p}_N^*)$, $\mathbf{p}_F$ is uniquely determined by $\mathbf{p}_L$.

For the tracking problem to be well posed, the affine transformation, and hence the desired positions of the followers, must be uniquely determined by the current positions of the leaders. For this purpose, the following lemma characterizes when a nominal formation is affinely localizable and specifies the conditions that the leaders' nominal positions must satisfy.

Lemma 1 ([10, Theorem 1]). *Assume that $\{\mathbf{p}_i^*\}_{i\in\mathcal{I}}$ affinely span $\mathbb{R}^d$. Then, the nominal formation is affinely localizable if and only if the nominal leaders' positions $\{\mathbf{p}_i^*\}_{i\in\mathcal{I}_L}$ affinely span $\mathbb{R}^d$.*

For the purpose of obtaining the concrete positions for the followers in terms of those of the leaders, the concept of the stress matrix $\overline{\mathbf{\Omega}} \in \mathbb{R}^{N\times N}$ is introduced, which has components

$$[\overline{\mathbf{\Omega}}]_{ij} = \begin{cases} 0 & \text{if } i \neq j, (i,j) \notin \mathcal{E} \\ -\omega_{ij} & \text{if } i \neq j, (i,j) \in \mathcal{E} \\ \sum\limits_{k\in\mathcal{N}_i} \omega_{ik} & \text{if } i = j \end{cases}.$$

with the weights ω_{ij} in $\overline{\mathbf{\Omega}}$ chosen such that

$$\sum_{j\in\mathcal{N}_i} \omega_{ij}(\mathbf{p}_i^* - \mathbf{p}_j^*) = 0, \forall i \in \mathcal{I}. \tag{1}$$

The existence of $\overline{\mathbf{\Omega}}$ for the formation guaranteeing (1) is ensured for a wide range of formations as studied in [10], in particular for those called *generically universally rigid* which satisfy that $\overline{\mathbf{\Omega}}$ is positive semidefinite. In addition, the steps used to compute $\overline{\mathbf{\Omega}}$ given the graph $\mathcal{G}$ and the nominal configuration are given in [10, Section VII.A]. The following lemma establishes a direct relation between the nullspace of $\overline{\mathbf{\Omega}}$ and the affine image of the nominal configuration:

Lemma 2 ([10, Adapted from Lemma 5]). *Consider a graph $\mathcal{G}$, a nominal formation $\{\mathbf{p}_i^*\}_{i\in\mathcal{I}}$ and their corresponding stress matrix $\overline{\mathbf{\Omega}}$, satisfying* $\operatorname{rank}(\overline{\mathbf{\Omega}}) = N - d - 1$. *Then, $\{\mathbf{p}_i^*\}_{i\in\mathcal{I}}$ affinely span $\mathbb{R}^d$ if and only if* $\operatorname{Null}(\overline{\mathbf{\Omega}} \otimes \mathbf{I}_d) = \mathcal{A}(\mathbf{p}_1^*, \ldots, \mathbf{p}_N^*)$, *where* $\operatorname{Null}(\bullet)$ *represents the nullspace of the input matrix $\bullet$.*

The following lemma gives the explicit relationship between the leaders' and followers' positions when the nominal formation is affinely localizable.

Lemma 3 ([10, Theorem 2]). *Let the conditions of Lemma 2 hold and*

$$\mathbf{\Omega} = \overline{\mathbf{\Omega}} \otimes \mathbf{I}_d$$

be decomposed as

$$\mathbf{\Omega} = \begin{bmatrix}\mathbf{\Omega}_{LL} & \mathbf{\Omega}_{LF} \\ \mathbf{\Omega}_{LF}^\top & \mathbf{\Omega}_{FF}\end{bmatrix}$$

where $\mathbf{\Omega}_{LL} \in \mathbb{R}^{d\cdot N_L \times d\cdot N_L}$ and the rest of the matrices are of appropriate dimension. Then, the nominal formation is affinely localizable if and only if $\mathbf{\Omega}_{FF}$ is nonsingular. Moreover, when $\mathbf{\Omega}_{FF}$ is nonsingular, for any $\mathbf{p} \in \mathcal{A}(\mathbf{p}_1^*, \ldots, \mathbf{p}_N^*)$, $\mathbf{p}_F$ can be uniquely determined as

$$\mathbf{p}_F = -\mathbf{\Omega}_{FF}^{-1}\mathbf{\Omega}_{LF}^\top \mathbf{p}_L.$$

Besides these results, we also make use of the standard comparison lemma [39, Lemma 3.4] as well as norm inequalities, which we reproduce here for clarity:

Lemma 4 (Adapted from [39, Lemma 3.4]). *Consider the scalar differential equation*:

$$\dot{x}(t) = f(t, x(t))$$

where $f(t,x) \in \mathbb{R}$ is continuous in t and locally Lipschitz in x for all $t \geq t_0 \geq 0$ and all $x \in \mathbb{R}$. Let $y(t)$ be a differentiable function that satisfies:

$$\dot{y}(t) \leq f(t, y(t))$$

with $y(t_0) \leq x(t_0)$. Then, $y(t) \leq x(t)$ for all $t \in [t_0, \infty)$.

Lemma 5 ([40, Theorem 19, Page 28]). *Let $\mathbf{v} = [v_1, \ldots, v_n]^T \in \mathbb{R}^n$ and define $\|\mathbf{v}\|_p = \left(\sum_{i=1}^n |v_i|^p\right)^{1/p}$. Then, with $0 < r < s$, it follows that $\|\mathbf{v}\|_s \leq \|\mathbf{v}\|_r$.*

3 | Observer-Based Affine Formation Tracking

In this work, we assume that the nominal formation is affinely localizable and that the trajectories of the leader agents

$$\mathbf{p}_L(t) = \begin{bmatrix}\mathbf{p}_1(t) \\ \vdots \\ \mathbf{p}_{N_L}(t)\end{bmatrix} \tag{2}$$

are exogenous time-varying signals. The followers are assumed to have dynamics of the form

$$\mathbf{p}_i^{(m_i)}(t) = \mathbf{u}_i(t), \quad i \in \mathcal{I}_F, \tag{3}$$

where $\mathbf{u}_i(t)$ is the local controller, m_i is the (possibly agent-dependent) relative degree, and $\mathbf{p}_i^{(m_i)}(t)$ denotes the m_i-th time derivative of $\mathbf{p}_i(t)$.

The objective is to design controllers $\mathbf{u}_i(t)$, based solely on shared local information, so that the followers' positions converge to the time-varying target configuration

$$\mathbf{p}_F(t) = \begin{bmatrix} \mathbf{p}_{N_L+1}(t) \\ \vdots \\ \mathbf{p}_N(t) \end{bmatrix} = -\mathbf{\Omega}_{FF}^{-1}\mathbf{\Omega}_{LF}^{\top}\mathbf{p}_L(t),$$

as determined by the leaders' current positions in Lemma 3. That is, we want

$$\lim_{t\to\infty} \left\| \mathbf{p}_F(t) - (-\mathbf{\Omega}_{FF}^{-1}\mathbf{\Omega}_{LF}^{\top}\mathbf{p}_L(t)) \right\| = 0. \tag{4}$$

To solve this problem, we adopt a hierarchical approach. First, each follower $i \in \mathcal{I}_F$ runs a local observer to estimate its target position and its derivatives from the leaders' current positions. Second, these estimates serve as reference signals in a trajectory-tracking controller for (3).

The proposed local HOSM observer of order $m \geq \max\{m_i\}_{i\in\mathcal{I}_F}$ stores $\{\hat{\mathbf{p}}_{i,\mu}(t)\}_{\mu=0}^{m}$ at each follower, where $\hat{\mathbf{p}}_{i,\mu}(t)$ is the estimate of the μ-th derivative of the target position. The observer updates are given by

$$\begin{aligned} \dot{\hat{\mathbf{p}}}_{i,\mu}(t) &= \hat{\mathbf{p}}_{i,\mu+1}(t) - \kappa_\mu \mathbf{f}_\mu\left(\sum_{j\in\mathcal{N}_i} \omega_{ij}\left(\hat{\mathbf{p}}_{i,\mu}(t) - \hat{\mathbf{p}}_{j,\mu}(t)\right)\right), \\ &\qquad \mu \in \{0, \ldots, m-1\}, \\ \dot{\hat{\mathbf{p}}}_{i,m}(t) &= -\kappa_m \mathbf{f}_m\left(\sum_{j\in\mathcal{N}_i} \omega_{ij}\left(\hat{\mathbf{p}}_{i,m}(t) - \hat{\mathbf{p}}_{j,m}(t)\right)\right), \end{aligned} \tag{5}$$

for a follower agent $i \in \mathcal{I}_F$ with arbitrary initial conditions, design parameters $\{\kappa_\mu\}_{\mu=0}^{m} > 0$, stress matrix entries ω_{ij}, and $\mathbf{f}_\mu(\bullet) = \lceil \bullet \rfloor^{\alpha_\mu}$ with $\alpha_\mu = \frac{m-\mu}{m-\mu+1}$. Note that for $\mu = m$, we have $\alpha_m = 0$, hence $\mathbf{f}_m(\bullet) = \lceil \bullet \rfloor^0 = \operatorname{sign}(\bullet)$ is discontinuous. For this reason, solutions of (5) are understood in the sense of Filippov [41]. As a result, differential inclusions will be used repeatedly in this work, as is standard in the study of sliding modes [15, 35].

For the leaders, we set

$$\hat{\mathbf{p}}_{i,\mu}(t) := \mathbf{p}_i^{(\mu)}(t), \quad i \in \mathcal{I}_L. \tag{6}$$

From (6), we assume that a leader $i \in \mathcal{I}_L$ has access to $\mathbf{p}_i^{(\mu)}(t)$ for $\mu \leq m$, which may not be directly available from sensors in practice. However, these can be estimated using only position measurements, as described in Section 5.1.

The leaders' states act as inputs to the followers' observers. We define

$$\hat{\mathbf{p}}_{F,\mu}(t) = \begin{bmatrix} \hat{\mathbf{p}}_{N_L+1,\mu}(t) \\ \vdots \\ \hat{\mathbf{p}}_{N,\mu}(t) \end{bmatrix}, \quad \hat{\mathbf{p}}_{\mu}(t) = \begin{bmatrix} \hat{\mathbf{p}}_{1,\mu}(t) \\ \vdots \\ \hat{\mathbf{p}}_{N_L,\mu}(t) \\ \hat{\mathbf{p}}_{N_L+1,\mu}(t) \\ \vdots \\ \hat{\mathbf{p}}_{N,\mu}(t) \end{bmatrix}, \tag{7}$$

which, using (2) and (6), yield

$$\hat{\mathbf{p}}_{\mu}(t) = \begin{bmatrix} \mathbf{p}_1^{(\mu)}(t) \\ \vdots \\ \mathbf{p}_{N_L}^{(\mu)}(t) \\ \hat{\mathbf{p}}_{N_L+1,\mu}(t) \\ \vdots \\ \hat{\mathbf{p}}_{N,\mu}(t) \end{bmatrix} = \begin{bmatrix} \mathbf{p}_L^{(\mu)}(t) \\ \hat{\mathbf{p}}_{F,\mu}(t) \end{bmatrix}. \tag{8}$$

where $\mathbf{p}_L^{(\mu)}(t)$ in (8) denotes the μ-th derivative of $\mathbf{p}_L(t)$. From a communication standpoint, $\mathcal{N}_i$ in (5) denotes the neighborhood of $i \in \mathcal{I}_F$ in $\mathcal{G}$, including both leaders and followers. Thus, follower i requires $\{\hat{\mathbf{p}}_{j,\mu}(t)\}_{\mu=0}^{m}$ from all $j \in \mathcal{N}_i$. Leaders share $\{\mathbf{p}_j^{(\mu)}(t)\}_{\mu=0}^{m}$ as per (6), while followers share their own locally computed $\{\hat{\mathbf{p}}_{j,\mu}(t)\}_{\mu=0}^{m}$.

Remark 1. The choice of α_μ in (5) ensures that the observer error system is weighted homogeneous, that is, invariant under the transformation $t' = \eta t$, $\boldsymbol{\delta}'_\mu(t') = \eta^{m-\mu+1}\boldsymbol{\delta}_\mu(t'/\eta)$ [35]. This property is used in Section 5 to establish robustness under measurement noise and discrete-time sampling.

Assumption 1 (Leader motion constraints). Assume that the nominal formation is affinely localizable, generically universally rigid, and that the exogenous leader positions $\mathbf{p}_L(t)$ have bounded $(m+1)$-th derivative, with

$$\mathbf{r}(t) = \mathbf{\Omega}_{FF}^{-1}\mathbf{\Omega}_{LF}^{\top}\mathbf{p}_L^{(m+1)}(t) \in [-B, B]^{d\cdot N_F}, \quad \forall t \geq 0,$$

for some known $B > 0$.

The only requirement in Assumption 1 is that the $(m+1)$-th derivative of $\mathbf{p}_L(t)$ be bounded by a known constant, which can be enforced as a constraint during trajectory planning. This condition is compatible with a wide variety of leader trajectories.

Theorem 1. *Let Assumption 1 hold,* $\kappa_\mu > 0$ *for* $\mu \in \{0, \ldots, m-1\}$, *and*

$$\kappa_m > B\sqrt{\frac{d \cdot N_F\ \sigma_{\max}(\mathbf{\Omega}_{FF})}{\sigma_{\min}(\mathbf{\Omega}_{FF})}}.$$

Then there exists $\mathcal{T} > 0$ *such that*

$$\hat{\mathbf{p}}_{F,\mu}(t) = -\mathbf{\Omega}_{FF}^{-1}\mathbf{\Omega}_{LF}^{\top}\mathbf{p}_L^{(\mu)}(t), \quad \forall t \geq \mathcal{T},\ \mu \in \{0, \ldots, m\}.$$

Proof. See Section 4.2. □

The design condition on κ_m in Theorem 1 depends on the singular values of $\mathbf{\Omega}_{FF}$. Moreover, the weights ω_{ij} in (5) generally require centralized computation, as in other affine formation control schemes [10, 13, 15]. These parameters can be computed and distributed through an initialization procedure.

Theorem 1 guarantees that, after a finite time, the followers can obtain their target positions and corresponding derivatives from the leaders' current positions via the outputs of the observer (5). From these outputs, each agent can implement a local trajectory tracking controller to follow its target position. For instance, design parameters $\{\rho_{i,\mu}\}_{\mu=0}^{m_i-1}$ can be chosen for a standard linear trajectory tracking controller, where the observer outputs $\hat{\mathbf{p}}_{i,\mu}(t)$ act as the reference signals at follower agent $i \in \mathcal{I}_F$:

$$\mathbf{u}_i(t) = \hat{\mathbf{p}}_{i,m_i}(t) - \sum_{\mu=0}^{m_i-1} \rho_{i,\mu}\left(\mathbf{p}_i^{(\mu)}(t) - \hat{\mathbf{p}}_{i,\mu}(t)\right). \tag{9}$$

Proposition 1. *Let Assumption 1 hold and (5) be designed as in Theorem 1. Moreover, let $\{\rho_{i,\mu}\}_{\mu=0}^{m_i-1}$ be chosen such that the polynomial $q(s) = s^{m_i} + \sum_{\mu=0}^{m_i-1}\rho_{i,\mu}s^{\mu}$ of complex variable s is Hurwitz for every $i \in \mathcal{I}_F$, meaning that all solutions s of $q(s) = 0$ have negative real part. Then, using (9) in (3) ensures that every follower asymptotically converges to its position in the target configuration as given in (4).*

Proof. Set the reference for the followers as

$$\mathbf{p}_{F,\mathrm{ref}}(t) = -\mathbf{\Omega}_{FF}^{-1}\mathbf{\Omega}_{LF}^{\top}\mathbf{p}_L(t) = \begin{bmatrix} \mathbf{p}_{N_L+1,\mathrm{ref}}(t) \\ \vdots \\ \mathbf{p}_{N,\mathrm{ref}}(t) \end{bmatrix},$$

and define the tracking error $\mathbf{e}_i(t) = \mathbf{p}_i(t) - \mathbf{p}_{i,\mathrm{ref}}(t)$ for $i \in \mathcal{I}_F$. Then,

$$\begin{aligned} \mathbf{e}_i^{(m_i)}(t) &= \mathbf{u}_i(t) - \mathbf{p}_{i,\mathrm{ref}}^{(m_i)}(t) \\ &= \hat{\mathbf{p}}_{i,m_i}(t) - \mathbf{p}_{i,\mathrm{ref}}^{(m_i)}(t) - \sum_{\mu=0}^{m_i-1}\rho_{i,\mu}\left(\mathbf{p}_i^{(\mu)}(t) - \hat{\mathbf{p}}_{i,\mu}(t)\right) \\ &= -\sum_{\mu=0}^{m_i-1}\rho_{i,\mu}\,\mathbf{e}_i^{(\mu)}(t) + \mathbf{d}_i(t), \end{aligned} \tag{10}$$

where

$$\mathbf{d}_i(t) = \left(\hat{\mathbf{p}}_{i,m_i}(t) - \mathbf{p}_{i,\mathrm{ref}}^{(m_i)}(t)\right) + \sum_{\mu=0}^{m_i-1}\rho_{i,\mu}\left(\hat{\mathbf{p}}_{i,\mu}(t) - \mathbf{p}_{i,\mathrm{ref}}^{(\mu)}(t)\right).$$

Since $\{\rho_{i,\mu}\}_{\mu=0}^{m_i-1}$ lead to a Hurwitz characteristic polynomial, (10) is BIBO stable with respect to $\mathbf{d}_i(t)$. By Theorem 1, $\mathbf{d}_i(t)$ is bounded, so regardless of the initial follower conditions $\mathbf{p}_i^{(\mu)}(0)$, $i \in \mathcal{I}_F$, the values of $\mathbf{p}_i^{(\mu)}(t)$ remain bounded for $t \in [0, \mathcal{T}]$ with $\mathcal{T}$ given in Theorem 1. Hence, there are no finite-time escapes before convergence of the observer (5). For $t \geq \mathcal{T}$, $\mathbf{d}_i(t) \equiv \mathbf{0}$, so (10) becomes disturbance-free and $\lim_{t\to\infty}\|\mathbf{e}_i(t)\| = 0$, completing the proof. □

Remark 2. From the proof of Proposition 1, it follows that any trajectory tracking controller that guarantees no finite-time escapes for the error system (10) can be used. Consequently, any BIBO-stable tracking controller is admissible. Since estimates of high-order derivatives of the target position are available to every follower, the approach allows considerable flexibility in the choice of follower dynamics and controllers. For example, it can be applied to agents with nonlinear dynamics using suitable tracking controllers for unicycle systems [42], multirotors [43], and Euler-Lagrange systems [44].

Remark 3. The proposed observer (5) requires agent positions to be expressed in a common global reference frame. This condition is met in many applications where absolute positioning is routinely available without centralized computation, such as outdoor multi-agent systems with GPS or indoor environments equipped with UWB, optical tracking, or other infrastructure-based localization systems. In settings without such infrastructure, a global frame can still be established in a distributed manner from relative measurements or a small set of anchors with known positions, using established distributed localization and coordinate alignment methods such as [45]. Once such a common frame is available, either through infrastructure or distributed estimation, the proposed scheme can be applied without modification.

4 | Observer Convergence Analysis

4.1 | Toward Convergence

This section presents several useful lemmas for the convergence proof of (5). First, write (5) in compact form:

$$\begin{aligned} \dot{\hat{\mathbf{p}}}_{F,\mu}(t) &= \hat{\mathbf{p}}_{F,\mu+1}(t) - \kappa_\mu\begin{bmatrix}\mathbf{0}_{d\cdot N_F\times d\cdot N_L} & \mathbf{I}_{d\cdot N_F}\end{bmatrix}\mathbf{f}_\mu(\mathbf{\Omega}\hat{\mathbf{p}}_\mu(t)) \\ &\qquad \text{for } \mu \in \{0,\ldots,m-1\} \\ \dot{\hat{\mathbf{p}}}_{F,m}(t) &= -\kappa_m\begin{bmatrix}\mathbf{0}_{d\cdot N_F\times d\cdot N_L} & \mathbf{I}_{d\cdot N_F}\end{bmatrix}\mathbf{f}_m(\mathbf{\Omega}\hat{\mathbf{p}}_m(t)). \end{aligned} \tag{11}$$

Denote the follower observation error by

$$\boldsymbol{\delta}_\mu(t) = \hat{\mathbf{p}}_{F,\mu}(t) + \mathbf{\Omega}_{FF}^{-1}\mathbf{\Omega}_{LF}^{\top}\mathbf{p}_L^{(\mu)}(t). \tag{12}$$

Convergence of (5) as described in Theorem 1 implies convergence of $\{\boldsymbol{\delta}_\mu(t)\}_{\mu=0}^{m}$ in finite time toward the origin, and the following result establishes the dynamics for this error.

Lemma 6. *Let Assumption 1 hold and consider system (5). Then, $\{\boldsymbol{\delta}_\mu(t)\}_{\mu=0}^{m}$ with $\boldsymbol{\delta}_\mu(t)$ in (12) satisfy*

$$\begin{aligned} \dot{\boldsymbol{\delta}}_\mu(t) &= \boldsymbol{\delta}_{\mu+1}(t) - \kappa_\mu\mathbf{f}_\mu(\mathbf{\Omega}_{FF}\boldsymbol{\delta}_\mu(t)), \quad \mu \in \{0,\ldots,m-1\} \\ \dot{\boldsymbol{\delta}}_m(t) &= \mathbf{r}(t) - \kappa_m\mathbf{f}_m(\mathbf{\Omega}_{FF}\boldsymbol{\delta}_m(t)). \end{aligned} \tag{13}$$

Proof. First, note that

$$\mathbf{\Omega}_{FF}\boldsymbol{\delta}_\mu(t) = \mathbf{\Omega}_{LF}^{\top}\mathbf{p}_L^{(\mu)}(t) + \mathbf{\Omega}_{FF}\hat{\mathbf{p}}_{F,\mu}(t) = \begin{bmatrix}\mathbf{\Omega}_{LF}^{\top} & \mathbf{\Omega}_{FF}\end{bmatrix}\hat{\mathbf{p}}_\mu(t). \tag{14}$$

Since Assumption 1 holds, Lemma 2 ensures

$$\begin{bmatrix}\mathbf{p}_L(t) \\ -\mathbf{\Omega}_{FF}^{-1}\mathbf{\Omega}_{LF}^{\top}\mathbf{p}_L(t)\end{bmatrix} \in \mathrm{Null}(\overline{\mathbf{\Omega}} \otimes \mathbf{I}_d).$$

Then,

$$\mathbf{0} = \boldsymbol{\Omega}\begin{bmatrix}\mathbf{p}_L(t)\\ -\boldsymbol{\Omega}_{FF}^{-1}\boldsymbol{\Omega}_{LF}^\top\mathbf{p}_L(t)\end{bmatrix} = \begin{bmatrix}\boldsymbol{\Omega}_{LL} & \boldsymbol{\Omega}_{LF}\\ \boldsymbol{\Omega}_{LF}^\top & \boldsymbol{\Omega}_{FF}\end{bmatrix}\begin{bmatrix}\mathbf{p}_L(t)\\ -\boldsymbol{\Omega}_{FF}^{-1}\boldsymbol{\Omega}_{LF}^\top\mathbf{p}_L(t)\end{bmatrix}$$
$$= \begin{bmatrix}\boldsymbol{\Omega}_{LL}\mathbf{p}_L(t) - \boldsymbol{\Omega}_{LF}\boldsymbol{\Omega}_{FF}^{-1}\boldsymbol{\Omega}_{LF}^\top\mathbf{p}_L(t)\\ \boldsymbol{\Omega}_{LF}^\top\mathbf{p}_L(t) - \boldsymbol{\Omega}_{FF}\boldsymbol{\Omega}_{FF}^{-1}\boldsymbol{\Omega}_{LF}^\top\mathbf{p}_L(t)\end{bmatrix}$$

which, taking μ-th time derivative, leads to

$$\boldsymbol{\Omega}_{LL}\mathbf{p}_L^{(\mu)}(t) = \boldsymbol{\Omega}_{LF}\boldsymbol{\Omega}_{FF}^{-1}\boldsymbol{\Omega}_{LF}^\top\mathbf{p}_L^{(\mu)}(t)$$

and therefore

$$\begin{aligned}&\begin{bmatrix}\boldsymbol{\Omega}_{LL} & \boldsymbol{\Omega}_{LF}\end{bmatrix}\hat{\mathbf{p}}_\mu(t) = \boldsymbol{\Omega}_{LL}\mathbf{p}_L^{(\mu)}(t) + \boldsymbol{\Omega}_{LF}\hat{\mathbf{p}}_{F,\mu}(t)\\ &= \boldsymbol{\Omega}_{LF}\boldsymbol{\Omega}_{FF}^{-1}\boldsymbol{\Omega}_{LF}^\top\mathbf{p}_L^{(\mu)}(t) + \boldsymbol{\Omega}_{LF}\hat{\mathbf{p}}_{F,\mu}(t)\\ &= \boldsymbol{\Omega}_{LF}\left(\boldsymbol{\Omega}_{FF}^{-1}\boldsymbol{\Omega}_{LF}^\top\mathbf{p}_L^{(\mu)}(t) + \hat{\mathbf{p}}_{F,\mu}(t)\right) = \boldsymbol{\Omega}_{LF}\boldsymbol{\delta}_\mu(t).\end{aligned} \tag{15}$$

Then, combining (14) and (15) we have that

$$\begin{bmatrix}\boldsymbol{\Omega}_{LF}\\ \boldsymbol{\Omega}_{FF}\end{bmatrix}\boldsymbol{\delta}_\mu(t) = \boldsymbol{\Omega}\hat{\mathbf{p}}_\mu(t). \tag{16}$$

As a result, we have that

$$\begin{aligned}&\begin{bmatrix}\mathbf{0}_{d\cdot N_F\times d\cdot N_L} & \mathbf{I}_{d\cdot N_F}\end{bmatrix}\mathbf{f}_\mu(\boldsymbol{\Omega}\hat{\mathbf{p}}_\mu(t))\\ &= \begin{bmatrix}\mathbf{0}_{d\cdot N_F\times d\cdot N_L} & \mathbf{I}_{d\cdot N_F}\end{bmatrix}\mathbf{f}_\mu\left(\begin{bmatrix}\boldsymbol{\Omega}_{LF}\\ \boldsymbol{\Omega}_{FF}\end{bmatrix}\boldsymbol{\delta}_\mu(t)\right)\\ &= \begin{bmatrix}\mathbf{0}_{d\cdot N_F\times d\cdot N_L} & \mathbf{I}_{d\cdot N_F}\end{bmatrix}\begin{bmatrix}\mathbf{f}_\mu(\boldsymbol{\Omega}_{LF}\boldsymbol{\delta}_\mu(t))\\ \mathbf{f}_\mu(\boldsymbol{\Omega}_{FF}\boldsymbol{\delta}_\mu(t))\end{bmatrix}\\ &= \mathbf{f}_\mu(\boldsymbol{\Omega}_{FF}\boldsymbol{\delta}_\mu(t)).\end{aligned}$$

Henceforth, for $\mu \in \{0, \dots, m-1\}$, using (11):

$$\begin{aligned}\dot{\boldsymbol{\delta}}_\mu(t) &= \boldsymbol{\Omega}_{FF}^{-1}\boldsymbol{\Omega}_{LF}^\top\mathbf{p}_L^{(\mu+1)}(t) + \dot{\hat{\mathbf{p}}}_{F,\mu}(t)\\ &= \boldsymbol{\Omega}_{FF}^{-1}\boldsymbol{\Omega}_{LF}^\top\mathbf{p}_L^{(\mu+1)}(t) + \hat{\mathbf{p}}_{F,\mu+1}(t)\\ &\quad - \kappa_\mu\begin{bmatrix}\mathbf{0}_{d\cdot N_F\times d\cdot N_L} & \mathbf{I}_{d\cdot N_F}\end{bmatrix}\mathbf{f}_\mu(\boldsymbol{\Omega}\hat{\mathbf{p}}_\mu(t))\\ &= \boldsymbol{\delta}_{\mu+1}(t) - \kappa_\mu\mathbf{f}_\mu(\boldsymbol{\Omega}_{FF}\boldsymbol{\delta}_\mu(t))\end{aligned}$$

and similarly, for $\mu = m$:

$$\begin{aligned}\dot{\boldsymbol{\delta}}_m(t) &= \boldsymbol{\Omega}_{FF}^{-1}\boldsymbol{\Omega}_{LF}^\top\mathbf{p}_L^{(m+1)}(t) + \dot{\hat{\mathbf{p}}}_{F,m}(t)\\ &= \boldsymbol{\Omega}_{FF}^{-1}\boldsymbol{\Omega}_{LF}^\top\mathbf{p}_L^{(m+1)}(t)\\ &\quad - \kappa_m\begin{bmatrix}\mathbf{0}_{d\cdot N_F\times d\cdot N_L} & \mathbf{I}_{d\cdot N_F}\end{bmatrix}\boldsymbol{\Omega}\mathbf{f}_m(\boldsymbol{\Omega}\hat{\mathbf{p}}_m(t))\\ &= \mathbf{r}(t) - \kappa_m\mathbf{f}_m(\boldsymbol{\Omega}_{FF}\boldsymbol{\delta}_m(t)).\end{aligned}$$

□

The following result establishes a Lyapunov inequality for an auxiliary system which will be useful to study (13).

Lemma 7. *Consider the differential inclusion*

$$\dot{\boldsymbol{\delta}}_\mu(t) \in [-B_\mu, B_\mu]^{d\cdot N_F} - \kappa_\mu\lceil\boldsymbol{\Omega}_{FF}\boldsymbol{\delta}_\mu(t)\rfloor^{\alpha_\mu} \tag{17}$$

for some $B_\mu \geq 0$ and $\alpha_\mu \in [0, 1)$. Then, $V_\mu(\boldsymbol{\delta}_\mu(t)) = \frac{1}{2}\boldsymbol{\delta}_\mu(t)^\top\boldsymbol{\Omega}_{FF}\boldsymbol{\delta}_\mu(t)$ is positive definite and satisfies

$$\dot{V}_\mu(\boldsymbol{\delta}_\mu(t)) \leq \gamma_\mu\sqrt{V_\mu(\boldsymbol{\delta}_\mu(t))} - \zeta_\mu V_\mu(\boldsymbol{\delta}_\mu(t))^{\frac{\alpha_\mu+1}{2}}$$

with $\gamma_\mu = B_\mu\sqrt{2d\cdot N_F\sigma_{\max}(\boldsymbol{\Omega}_{FF})}$ *and* $\zeta_\mu = 2^{\frac{\alpha_\mu+1}{2}}\kappa_\mu\sigma_{\min}(\boldsymbol{\Omega}_{FF})^{\frac{\alpha_\mu+1}{2}}$.

Proof. First, note that due to Assumption 1, the nominal formation is generically universally rigid. Hence, $\boldsymbol{\Omega}$ is positive semidefinite and thus its principal block $\boldsymbol{\Omega}_{FF}$ is as well. Moreover, the formation is affinely localizable and thus Lemma 3 implies $\boldsymbol{\Omega}_{FF}$ is nonsingular. As a result, $\boldsymbol{\Omega}_{FF}$ is positive definite. Henceforth, $V_\mu(\boldsymbol{\delta}_\mu(t))$ is positive definite as well. Moreover, it satisfies that for any $\mathbf{r}_\mu(t) \in [-B_\mu, B_\mu]^{d\cdot N_F}$:

$$\begin{aligned}\dot{V}_\mu(\boldsymbol{\delta}_\mu(t)) &= \boldsymbol{\delta}_\mu(t)^\top\boldsymbol{\Omega}_{FF}\dot{\boldsymbol{\delta}}_\mu(t)\\ &= \boldsymbol{\delta}_\mu(t)^\top\boldsymbol{\Omega}_{FF}\mathbf{r}_\mu(t) - \kappa_\mu\boldsymbol{\delta}_\mu(t)^\top\boldsymbol{\Omega}_{FF}\lceil\boldsymbol{\Omega}_{FF}\boldsymbol{\delta}_\mu(t)\rfloor^{\alpha_\mu}\\ &\leq \|\mathbf{v}(t)\|\|\mathbf{r}_\mu(t)\| - \kappa_\mu\mathbf{v}(t)^\top\lceil\mathbf{v}(t)\rfloor^{\alpha_\mu}\\ &\leq B_\mu\sqrt{d\cdot N_F}\|\mathbf{v}(t)\| - \kappa_\mu\mathbf{v}(t)^\top\lceil\mathbf{v}(t)\rfloor^{\alpha_\mu}\end{aligned}$$

where $\mathbf{v}(t) = \boldsymbol{\Omega}_{FF}\boldsymbol{\delta}_\mu(t)$. Note that if $\mathbf{v}(t) = [v_1(t), \dots, v_{d\cdot N_F}(t)]^\top$ then

$$\mathbf{v}(t)^\top\lceil\mathbf{v}(t)\rfloor^{\alpha_\mu}\begin{bmatrix}v_1(t) & \dots & v_{dN}(t)\end{bmatrix}\begin{bmatrix}|v_1(t)|^{\alpha_\mu}\operatorname{sign}(v_1(t))\\ \vdots\\ |v_{dN}(t)|^{\alpha_\mu}\operatorname{sign}(v_{dN}(t))\end{bmatrix}$$
$$= (\|\mathbf{v}(t)\|_{\alpha_\mu+1})^{\alpha_\mu+1}$$

with the norm definition $(\|\mathbf{v}(t)\|_{\alpha_\mu+1})^{\alpha_\mu+1} = \sum_{k=1}^{d\cdot N_F}|v_k(t)|^{\alpha_\mu+1}$. Moreover,

$$\sigma_{\min}(\boldsymbol{\Omega}_{FF})\boldsymbol{\delta}_\mu^\top\boldsymbol{\Omega}_{FF}\boldsymbol{\delta}_\mu \leq \|\mathbf{v}(t)\|^2 \leq \sigma_{\max}(\boldsymbol{\Omega}_{FF})\boldsymbol{\delta}_\mu^\top\boldsymbol{\Omega}_{FF}\boldsymbol{\delta}_\mu.$$

Hence, Lemma 5, namely $\|\mathbf{v}\|_s \leq \|\mathbf{v}\|_r$ with $0 < r < s$, implies

$$\|\mathbf{v}(t)\|_{\alpha_\mu+1} \geq \|\mathbf{v}(t)\| \geq \sqrt{\sigma_{\min}(\boldsymbol{\Omega}_{FF})\boldsymbol{\delta}_\mu^\top(t)\boldsymbol{\Omega}_{FF}\boldsymbol{\delta}_\mu(t)}$$

due to $\alpha_\mu + 1 < 2$. Therefore:

$$\begin{aligned}\dot{V}_\mu(\boldsymbol{\delta}_\mu(t)) &\leq B_\mu\sqrt{d\cdot N_F}\|\mathbf{v}(t)\| - \kappa_\mu(\|\mathbf{v}(t)\|_{\alpha_\mu+1})^{\alpha_\mu+1}\\ &\leq B_\mu\sqrt{d\cdot N_F\sigma_{\max}(\boldsymbol{\Omega}_{FF})}\sqrt{\boldsymbol{\delta}_\mu^\top(t)\boldsymbol{\Omega}_{FF}\boldsymbol{\delta}_\mu(t)}\\ &\quad - \kappa_\mu\sigma_{\min}(\boldsymbol{\Omega}_{FF})^{\frac{\alpha_\mu+1}{2}}(\boldsymbol{\delta}_\mu^\top(t)\boldsymbol{\Omega}_{FF}\boldsymbol{\delta}_\mu(t))^{\frac{\alpha_\mu+1}{2}}\\ &= B_\mu\sqrt{d\cdot N_F\sigma_{\max}(\boldsymbol{\Omega}_{FF})}\sqrt{2V_\mu}\\ &\quad - \kappa_\mu\sigma_{\min}(\boldsymbol{\Omega}_{FF})^{\frac{\alpha_\mu+1}{2}}(2V_\mu)^{\frac{\alpha_\mu+1}{2}}\end{aligned}$$

completing the proof. □

Lemma 8. *Let $\dot{v}(t) = \eta_\mu\lceil v(t)\rfloor^{\beta_\mu}$ with $\beta_\mu \in [0, 1)$, $\mathcal{T}_\mu = \frac{|v(\tau)|^{1-\beta_\mu}}{(1-\beta_\mu)\eta_\mu}$ and initial time $\tau \geq 0$. Then,*

$$v(t)^{1-\beta_\mu} = \begin{cases}|v(\tau)|^{1-\beta_\mu} + (1-\beta_\mu)\eta_\mu(t-\tau) & \text{if } \eta_\mu \geq 0, t \geq \tau\\ |v(\tau)|^{1-\beta_\mu} - (1-\beta_\mu) & \text{if } \eta_\mu < 0,\\ \quad |\eta_\mu|(t-\tau) & t \in [\tau, \tau+\mathcal{T}_\mu]\\ 0 & \text{if } \eta_\mu < 0, t \geq \mathcal{T}_\mu + \tau\end{cases}.$$

Proof. It can be verified that the solution of the separable differential equation can be written as

$$|v(t)|^{1-\beta_\mu} = |v(\tau)|^{1-\beta_\mu} + (1-\beta_\mu)\eta_\mu(t-\tau)$$

for $v(t) \neq 0$ from which the case with $\eta_\mu \geq 0, t \geq \tau$ follows directly. Moreover, choose $V_v(v(t)) = v(t)^2/2$ such that

$$\dot{V}_v = \eta_\mu v(t)\lceil v(t)\rfloor^{\beta_\mu} = \eta_\mu |v(t)|^{\beta_\mu+1} < 0$$

for $v(t) \neq 0$ when $\eta_\mu < 0$. Henceforth, when $\eta_\mu < 0$ the origin is asymptotically stable. In this case, the explicit solution reaches the origin at $t = \tau + \mathcal{T}_\mu$ and remains there forever completing the proof. □

4.2 | Convergence of the Distributed Observer

Proof of Theorem 1. We will show, by induction, that there exist b_μ, τ_μ such that $\|\boldsymbol{\delta}_\mu(t)\| \leq b_\mu$ for $t \in [0, \tau_\mu]$ and $\boldsymbol{\delta}_\mu(t) = \mathbf{0}$ for $t \geq \tau_\mu$. As induction base, we start with $\mu = m$. Note that according to Lemma 6, $\dot{\boldsymbol{\delta}}_m(t)$ satisfy (17) with $B_m = B$ due to Assumption 1. Hence, Lemma 7 implies that $V_m(\boldsymbol{\delta}_m(t))$ satisfies

$$\begin{aligned}\dot{V}_m(\boldsymbol{\delta}_m(t)) &\leq \gamma_m\sqrt{V_m(\boldsymbol{\delta}_m(t))} - \zeta_m V_m(\boldsymbol{\delta}_m(t))^{\frac{\alpha_m+1}{2}} \\ &= \eta_m\sqrt{V_m(\boldsymbol{\delta}_m(t))}\end{aligned}$$

due to $\alpha_m = 0$ and with $\eta_m = \gamma_m - \zeta_m < 0$ due to the design conditions for κ_m in Theorem 1. Now we use the comparison Lemma 4 and Lemma 8 with $\mu = m, \beta_m = 1/2, \tau = 0$ to obtain

$$\sqrt{V_m(\boldsymbol{\delta}_m(t))} \leq \sqrt{V_m(\boldsymbol{\delta}_m(0))} - |\eta_m|t/2$$

if $t \in [0, \mathcal{T}_m]$ and $\sqrt{V_m(\boldsymbol{\delta}_m(t))} = 0$ for $t \geq \mathcal{T}_m$ with $\mathcal{T}_m > 0$ as in Lemma 8. Hence, the induction base is established with $\tau_m = \mathcal{T}_m$ and

$$b_m = \sqrt{2V_m(\boldsymbol{\delta}(0))/\sigma_{\min}(\boldsymbol{\Omega}_{FF})}.$$

Now, assume the induction hypothesis for $\boldsymbol{\delta}_{\mu+1}(t)$ in order to show it for $\boldsymbol{\delta}_\mu(t)$ for arbitrary $\mu \in \{0, \ldots, m-1\}$. This is, we assume the existence of $b_{\mu+1}, \tau_{\mu+1}$ such that $\|\boldsymbol{\delta}_{\mu+1}(t)\| \leq b_{\mu+1}$ for $t \in [0, \tau_{\mu+1}]$ and $\boldsymbol{\delta}_{\mu+1}(t) = \mathbf{0}$ for $t \geq \tau_{\mu+1}$. Under this setting, Lemma 6 implies that $\dot{\boldsymbol{\delta}}_\mu(t)$ satisfy (13), which is of the form (17), with $B_\mu = b_{\mu+1}$ for $t \in [0, \tau_{\mu+1}]$. Hence, in this interval, Lemma 7 implies that $V_\mu(\boldsymbol{\delta}_\mu(t))$ satisfy

$$\dot{V}_\mu(\boldsymbol{\delta}_\mu(t)) \leq \gamma_\mu\sqrt{V_\mu(\boldsymbol{\delta}_\mu(t))}$$

with $\gamma_\mu = b_{\mu+1}\sqrt{2d \cdot N_F\sigma_{\max}(\boldsymbol{\Omega}_{FF})}$. By the comparison Lemma 4 and Lemma 8 with $\eta_\mu = \gamma_\mu \geq 0, \beta_\mu = 1/2, \tau = 0$:

$$\begin{aligned}\sqrt{V_\mu(\boldsymbol{\delta}_\mu(t))} &\leq \sqrt{V_\mu(\boldsymbol{\delta}_\mu(0))} + \eta_\mu t/2 \leq \sqrt{V_\mu(\boldsymbol{\delta}_\mu(0))} + \eta_\mu\tau_{\mu+1}/2 \\ &=: b_\mu\sqrt{\sigma_{\min}(\boldsymbol{\Omega}_{FF})/2}\end{aligned}$$

for $t \in [0, \tau_{\mu+1}]$. Now, for $t \geq \tau_{\mu+1}$, if follows by the induction hypothesis that $\dot{\boldsymbol{\delta}}_\mu(t)$ satisfy (13), which is of the form (17), with $B_\mu = 0$. From Lemma 7, $V_\mu(\boldsymbol{\delta}_\mu(t))$ satisfy

$$\dot{V}_\mu(\boldsymbol{\delta}_\mu(t)) \leq -\zeta_\mu V_\mu(\boldsymbol{\delta}_\mu(t))^{\frac{\alpha_\mu+1}{2}} = \eta_\mu V_\mu(\boldsymbol{\delta}_\mu(t))^{\beta_\mu}$$

with $\eta_\mu = -\zeta_\mu < 0$ and $\beta_\mu = (\alpha_\mu + 1)/2$ for all $t \geq \tau_{\mu+1}$. From here, it follows that

$$\sqrt{\|\boldsymbol{\delta}_\mu(t)\|^2\sigma_{\min}(\boldsymbol{\Omega}_{FF})/2} \leq \sqrt{V_\mu(\boldsymbol{\delta}_\mu(t))} \leq b_\mu\sqrt{\sigma_{\min}(\boldsymbol{\Omega}_{FF})/2}$$

is maintained $\forall t \geq \tau_{\mu+1}$ since $V_\mu(\boldsymbol{\delta}_\mu(t))$ is nonincreasing in that interval. Moreover, the comparison Lemma 8 in addition to Lemma 8 with $\tau = \tau_{\mu+1}$ imply the existence of $\mathcal{T}_\mu > \tau_{\mu+1}$ such that $V_\mu(\boldsymbol{\delta}(t)) = 0$ for all $t \geq \mathcal{T}_\mu$. Hence, set $\tau_\mu = \mathcal{T}_\mu$ to complete the induction. Therefore, $\boldsymbol{\delta}_\mu(t) = \mathbf{0}, \forall \mu \in \{0, \ldots, m\}, \forall t \geq \mathcal{T} := \tau_0$.

5 | Robustness Analysis

5.1 | Robustness to Noisy Leader Measurements

Up to this point, it was assumed that a subset of the follower agents had access to leaders positions $\mathbf{p}_i(t)$ for some $i \in \mathcal{I}_L$, and their derivatives. In practice, follower agents may measure these quantities by means of onboard sensors or the leaders might communicate them directly. In any case, it is usual to have access to the position measurement $\mathbf{p}_i(t)$ but not directly to its derivatives. Hence, we study this usual scenario next in which the derivatives need to be estimated, providing a specific approach to carry out such estimation. If a leader node $i \in \mathcal{I}_L$ cooperates, has access to noisy measurements of its own position $\mathbf{p}_i^\varepsilon(t) = \mathbf{p}_i(t) + \boldsymbol{\varepsilon}_i(t)$ with noise $\boldsymbol{\varepsilon}_i(t) \in \varepsilon[-1, 1]^d$, it can replace (6) with the following derivative estimator:

$$\begin{aligned}\dot{\hat{\mathbf{p}}}_{i,\mu}(t) &= \hat{\mathbf{p}}_{i,\mu+1}(t) - \kappa_\mu^d\left\lceil\hat{\mathbf{p}}_{i,0}(t) - \mathbf{p}_i^\varepsilon(t)\right\rfloor^{\frac{m-\mu}{m+1}} \\ &\qquad \text{for } \mu \in \{0, \ldots, m-1\} \\ \dot{\hat{\mathbf{p}}}_{i,m}(t) &= -\kappa_m^d\left\lceil\hat{\mathbf{p}}_{i,0}(t) - \mathbf{p}_i^\varepsilon(t)\right\rfloor^{\frac{m-\mu}{m+1}}\end{aligned} \tag{18}$$

for $i \in \mathcal{I}_L$. The estimator in (18) corresponds to the Robust Exact Differentiator (RED) in [34] and will be used for the leaders in conjunction with (5) for the followers. Appropriate parameters $\{\kappa_\mu^d\}_{\mu=0}^m$ are known for the RED to induce the terminal neighborhoods

$$\|\hat{\mathbf{p}}_{i,\mu}(t) - \mathbf{p}_i^{(\mu)}(t)\| \leq c_\mu^d\varepsilon^{\frac{m-\mu+1}{m+1}} \tag{19}$$

for $i \in \mathcal{I}_L$, after some finite time $\mathcal{T}^d > 0$ and for positive constants $\{c_\mu^d\}_{\mu=0}^m$, provided $\mathbf{p}_i^{(m+1)}(t), i \in \mathcal{I}_L$ is uniformly bounded for all time. Note from (19) that (6) is recovered when $\varepsilon = 0$. In a case where the leader agents do not cooperate and cannot communicate directly with any follower, then some of the followers might measure the positions $\mathbf{p}_i^\varepsilon(t)$ and run a copy of (18) for every $i \in \mathcal{I}_L$. The following result establishes the robustness of the proposed observer (5) to measurement noise, when used in conjunction with (18).

Proposition 2. *Let the same assumptions as in Theorem 1 hold. Moreover, let (5) with (18) in place of (6). Then, there exists $\mathcal{T}_\gamma > 0$ and positive constants $\{\gamma_\mu\}_{\mu=0}^m$ such that for all $t \geq \mathcal{T}_\gamma$ and $\mu \in \{0, \ldots, m\}$:*

$$\left\|\hat{\mathbf{p}}_{F,\mu}(t) - \left(-\boldsymbol{\Omega}_{FF}^{-1}\boldsymbol{\Omega}_{LF}^\top\mathbf{p}_L^{(\mu)}(t)\right)\right\| \leq \gamma_\mu\varepsilon^{\frac{m-\mu+1}{m+1}}$$

Proof. Finite time escapes of (5) cannot occur before the convergence time of (18) at $t = \mathcal{T}^d$, even under noise using the same argument as in the proof for the standard differentiator in [34, Lemma 7]. Thus, we analyze $t \geq \mathcal{T}^d$. Let $\boldsymbol{\varepsilon}_\mu(t) = \hat{\mathbf{p}}_{L,\mu}(t) - \mathbf{p}_L^{(\mu)}(t)$ for $i \in \mathcal{I}_L$ with $\hat{\mathbf{p}}_{L,\mu}(t) = [\hat{\mathbf{p}}_{1,\mu}(t)^\top, \ldots, \hat{\mathbf{p}}_{N_L,\mu}(t)^\top]^\top$ Moreover, write

$$\hat{\mathbf{p}}_\mu(t) := \begin{bmatrix} \hat{\mathbf{p}}_{L,\mu}(t) \\ \hat{\mathbf{p}}_{F,\mu}(t) \end{bmatrix} = \begin{bmatrix} \mathbf{p}_L^{(\mu)}(t) \\ \hat{\mathbf{p}}_{F,\mu}(t) \end{bmatrix} + \begin{bmatrix} \boldsymbol{\varepsilon}_\mu(t) \\ \mathbf{0} \end{bmatrix}$$

in place of (7). The analogue version of (16) is:

$$\begin{aligned} \boldsymbol{\Omega}\hat{\mathbf{p}}_\mu(t) &= \boldsymbol{\Omega}\begin{bmatrix} \mathbf{p}_L^{(\mu)}(t) \\ \hat{\mathbf{p}}_{F,\mu}(t) \end{bmatrix} + \begin{bmatrix} \boldsymbol{\Omega}_{LL} & \boldsymbol{\Omega}_{LF} \\ \boldsymbol{\Omega}_{LF}^\top & \boldsymbol{\Omega}_{FF} \end{bmatrix}\begin{bmatrix} \boldsymbol{\varepsilon}_\mu(t) \\ \mathbf{0} \end{bmatrix} \\ &= \begin{bmatrix} \boldsymbol{\Omega}_{LF} \\ \boldsymbol{\Omega}_{FF} \end{bmatrix}\boldsymbol{\delta}_\mu(t) + \begin{bmatrix} \boldsymbol{\Omega}_{LL} \\ \boldsymbol{\Omega}_{LF}^\top \end{bmatrix}\boldsymbol{\varepsilon}_\mu(t). \end{aligned}$$

Henceforth,

$$\begin{aligned} \dot{\boldsymbol{\delta}}_\mu(t) &= \boldsymbol{\delta}_{\mu+1}(t) - \kappa_\mu \mathbf{f}_\mu\big(\boldsymbol{\Omega}_{FF}\boldsymbol{\delta}_\mu(t) + \boldsymbol{\Omega}_{LF}^\top\boldsymbol{\varepsilon}_\mu(t)\big),\ \mu \leq m-1 \\ \dot{\boldsymbol{\delta}}_m(t) &= \mathbf{r}(t) - \kappa_m\boldsymbol{\Omega}\mathbf{f}_m\big(\boldsymbol{\Omega}_{FF}\boldsymbol{\delta}_m(t) + \boldsymbol{\Omega}_{LF}^\top\boldsymbol{\varepsilon}_m(t)\big). \end{aligned} \tag{20}$$

Moreover, $\boldsymbol{\varepsilon}_\mu(t) \in [-1,1]^{d\cdot N_L}\sqrt{d\cdot N_L}c_\mu^d\varepsilon^{\frac{m-\mu+1}{m+1}}$ as a result of (19) for $t \geq \mathcal{T}^d$. Therefore, $\boldsymbol{\varepsilon}_\mu(t) \in [-1,1]^{d\cdot N_L}\rho^{m-\mu+1}$ with $\rho = \max_{0\leq\mu\leq m}\left(\sqrt{d\cdot N_L}c_\mu^d\right)^{\frac{1}{m-\mu+1}}\varepsilon^{\frac{1}{m+1}}$. It can be verified that (20) is invariant under the homogeneity transformation $t' = \eta t$, $\rho' = \eta\rho$, $\boldsymbol{\delta}'_\mu(t') = \eta^{m-\mu+1}\boldsymbol{\delta}_\mu(t'/\eta)$ with $\eta > 0$ following the same steps as in [36, Lemma 17]. Moreover, (20) is globally finite-time stable when $\rho = 0$ due to Theorem 1. Therefore, the result follows from [35, Theorem 2]. □

Remark 4. Note that in this section, noise is considered for $\hat{\mathbf{p}}_{i,\mu}(t)$ in (5) for the leader variables $i \in \mathcal{I}_L$ and not for followers $i \in \mathcal{I}_F$. The reason is that noise appears in practice due to measuring the leader positions. In contrast, $\hat{\mathbf{p}}_{i,\mu}(t)$ for followers $i \in \mathcal{I}_F$ are virtual variables stored digitally at each agent, and do not suffer from any additional noise. However, measurement noise for the follower position will impact the controller (e.g., the one in (9)) rather than the observer. Fortunately, since our scheme makes the design of the controller independent of the observer structure, additional analysis can be conducted individually using standard techniques, which we omit for conciseness.

5.2 | Robustness to Discrete-Time Communication

In the previous sections, continuous-time communication is assumed for the local observer in (5). However, implementation is made in discrete time. This makes the analysis of robustness to discrete-time communication particularly relevant. Assume that agents exchange messages at discrete time instants $\{k\Delta\}_{k=0}^\infty$ with sampling step $\Delta > 0$. Then, the alternative version of (5) is:

$$\begin{aligned} \hat{\mathbf{p}}_{i,\mu}[k+1] = \sum_{\nu=0}^{m-\mu}\Bigg(&\frac{\Delta^\nu}{\nu!}\hat{\mathbf{p}}_{i,\mu+\nu}[k] - \frac{\Delta^{\nu+1}\kappa_{\mu+\nu}}{(\nu+1)!} \\ &\times \mathbf{f}_{\mu+\nu}\Bigg(\sum_{j\in\mathcal{N}_i}\omega_{ij}(\hat{\mathbf{p}}_{i,\mu+\nu}[k] - \hat{\mathbf{p}}_{j,\mu+\nu}[k])\Bigg)\Bigg) \end{aligned} \tag{21}$$

for follower agents $i \in \mathcal{I}_F$, where we write $\hat{\mathbf{p}}_{i,\mu}[k] := \hat{\mathbf{p}}_{i,\mu}(k\Delta)$. Hence, information and updates are only produced at the discrete time instants $\{k\Delta\}_{k=0}^\infty$. Similarly as with (5), a leader $j \in \mathcal{I}_L$ shares $\{\hat{\mathbf{p}}_{j,\mu}[k]\}_{\mu=0}^m = \{\mathbf{p}_j^{(\mu)}[k]\}_{\mu=0}^m$ with its neighbors, whereas a follower $j \in \mathcal{I}_F$ shares $\{\hat{\mathbf{p}}_{j,\mu}[k]\}_{\mu=0}^m$ directly from its local version of (21).

The following result quantifies the chattering of the proposal, that is, the accuracy as a function of Δ and m.

Proposition 3. *Let the same assumptions as in Theorem 1 hold and consider (21). Then, there exists $K \in \mathbb{N}$ and positive constants $\{\gamma_\mu\}_{\mu=0}^m$ such that for all $k \geq K$:*

$$\left\|\hat{\mathbf{p}}_{F,\mu}[k] - \left(-\boldsymbol{\Omega}_{FF}^{-1}\boldsymbol{\Omega}_{LF}^\top\mathbf{p}_L^{(\mu)}[k]\right)\right\| \leq \gamma_\mu\Delta^{m-\mu+1}.$$

Proof. First, it can be verified that

$$\begin{aligned} \hat{\mathbf{p}}_{i,\mu}(t) = \sum_{\nu=0}^{m-\mu}\Bigg(&\frac{(t-k\Delta)^\nu}{\nu!}\hat{\mathbf{p}}_{i,\mu+\nu}[k] - \frac{(t-k\Delta)^{\nu+1}\kappa_{\mu+\nu}}{(\nu+1)!} \\ &\times \mathbf{f}_{\mu+\nu}\Bigg(\sum_{j\in\mathcal{N}_i}\omega_{ij}(\hat{\mathbf{p}}_{i,\mu+\nu}[k] - \hat{\mathbf{p}}_{j,\mu+\nu}[k])\Bigg)\Bigg) \end{aligned} \tag{22}$$

comply (21) and

$$\begin{aligned} \dot{\hat{\mathbf{p}}}_{i,\mu}(t) &= \hat{\mathbf{p}}_{i,\mu+1}(t) - \kappa_\mu\mathbf{f}_\mu\Bigg(\sum_{j\in\mathcal{N}_i}\omega_{ij}(\hat{\mathbf{p}}_{i,\mu}[k] - \hat{\mathbf{p}}_{j,\mu}[k])\Bigg) \\ &\qquad \text{for } \mu \in \{0,\ldots,m-1\} \\ \dot{\hat{\mathbf{p}}}_{i,m}(t) &= -\kappa_m\mathbf{f}_m\Bigg(\sum_{j\in\mathcal{N}_i}\omega_{ij}(\hat{\mathbf{p}}_{i,m}[k] - \hat{\mathbf{p}}_{j,m}[k])\Bigg). \end{aligned}$$

Henceforth, the error variables $\boldsymbol{\delta}_\mu(t)$ for (22) satisfy

$$\begin{aligned} \dot{\boldsymbol{\delta}}_\mu(t) &\in \boldsymbol{\delta}_{\mu+1}(t) - \kappa_\mu\mathbf{f}_\mu\big(\boldsymbol{\Omega}_{FF}\boldsymbol{\delta}_\mu(t-\Delta[0,1])\big),\ \mu \leq m-1 \\ \dot{\boldsymbol{\delta}}_m(t) &\in [-B,B]^{d\cdot N_F} - \kappa_\mu\mathbf{f}_m\big(\boldsymbol{\Omega}_{FF}\boldsymbol{\delta}_m(t-\Delta[0,1])\big) \end{aligned} \tag{23}$$

since

$$\boldsymbol{\delta}_\mu[k] = \boldsymbol{\delta}_\mu(t-(t-k\Delta)) \in \boldsymbol{\delta}_\mu(t-\Delta[0,1])$$

due to $t - k\Delta \in [0,\Delta]$ when $t \in [k\Delta,(k+1)\Delta]$. It can be verified that (23) is invariant under the homogeneity transformation $t' = \eta t$, $\rho' = \eta\rho$, $\boldsymbol{\delta}'_\mu(t') = \eta^{m-\mu+1}\boldsymbol{\delta}_\mu(t'/\eta)$ with $\eta > 0$ and $\rho = \Delta$. Thus, the proof follows as in Proposition 2. □

For clarity, Proposition 2 and Proposition 3 separately addressed robustness to measurement noise and to discrete-time implementation. For completeness, the following result establishes convergence when both measurement noise and discrete-time updates are present simultaneously.

Corollary 1. *Let the same assumptions as in Theorem 1 hold. Moreover, let discrete-time noisy leader measurements $\hat{\mathbf{p}}_{i,\mu}(t), i \in \mathcal{I}_L$ complying*

$$\|\hat{\mathbf{p}}_{i,\mu}[k] - \mathbf{p}_i^{(\mu)}[k]\| \leq c_\mu^d\max\left\{\Delta,\varepsilon^{\frac{1}{m+1}}\right\}^{m-\mu+1} \tag{24}$$

for $i \in \mathcal{I}_L, \Delta, \varepsilon \geq 0$, for $k \geq K^d$ with finite time $K^d > 0$ and positive constants $\{c_\mu^d\}_{\mu=0}^m$. Hence, with such modification, there exists $K \in \mathbb{N}$ and positive constants $\{\gamma_\mu\}_{\mu=0}^m$ such that (21) complies that for all $k \geq K$:

$$\left\| \hat{\mathbf{p}}_{F,\mu}[k] - \left(-\boldsymbol{\Omega}_{FF}^{-1} \boldsymbol{\Omega}_{LF}^\top \mathbf{p}_L^{(\mu)}[k] \right) \right\| \leq \gamma_\mu \max \left\{ \Delta, \varepsilon^{\frac{1}{m+1}} \right\}^{m-\mu+1}$$

Proof. Assume $k \geq K^d$, condition after which (24) has been established. Follow the same arguments as in the proofs of Proposition 2 and Proposition 3 to obtain the error system:

$$\begin{aligned} \dot{\boldsymbol{\delta}}_\mu(t) &\in \boldsymbol{\delta}_{\mu+1}(t) - \kappa_\mu \mathbf{f}_\mu \left(\boldsymbol{\Omega}_{FF} \boldsymbol{\delta}_\mu(t - \rho[0,1]) + \boldsymbol{\Omega}_{LF}^\top \boldsymbol{\varepsilon}_\mu(t) \right), \mu \leq m-1 \\ \dot{\boldsymbol{\delta}}_m(t) &\in [-B, B]^{d \cdot N_F} - \kappa_\mu \mathbf{f}_m \left(\boldsymbol{\Omega}_{FF} \boldsymbol{\delta}_m(t - \rho[0,1]) + \boldsymbol{\Omega}_{LF}^\top \boldsymbol{\varepsilon}_m(t) \right) \end{aligned} \tag{25}$$

with $\boldsymbol{\varepsilon}_\mu(t) \in [-1,1]^{d \cdot N_L} \rho^{m-\mu+1}$ and

$$\rho = \max \left\{ \max_{0 \leq \mu \leq m} \left(\sqrt{d \cdot N_L} c_\mu^d \right)^{\frac{1}{m-\mu+1}} \max \left\{ \Delta, \varepsilon^{\frac{1}{m+1}} \right\}, \Delta \right\}.$$

Compare (25) with (20) and (23). It can be verified that (25) is invariant under the homogeneity transformation $t' = \eta t, \quad \rho' = \eta \rho, \quad \boldsymbol{\delta}'_\mu(t') = \eta^{m-\mu+1} \boldsymbol{\delta}_\mu(t'/\eta)$ with $\eta > 0$. Hence, the proof follows in the same way as in Proposition 2 and Proposition 3. □

Remark 5. The terminal bounds obtained in Corollary 1 rely on noisy leader measurements with accuracies of the form (24), rather than directly on the continuous-time differentiator (18). Nevertheless, [46] presents a discretization method for simulating (18) that guarantees precisely the accuracy requirement in (24), provided that $\mathbf{p}_i^{(m+1)}(t), i \in \mathcal{I}_L$, is uniformly bounded for all time.

6 | Numerical Examples

For the sake of conciseness, we consider the nominal formation and stress matrix borrowed from the example in [10, Figure 3] with $N = 7$ and $d = 2$. We set $N_L = 3$. All noise signal components were simulated by drawing uniformly in $\varepsilon[-1,1]$ for each t, with ε described for each experiment. To test persistently varying leader trajectories for all experiments, these are selected as

$$\begin{aligned} \mathbf{p}_i(t) &= \begin{bmatrix} 2\cos(t) & \sin(t) \\ \sin(t) & 2\cos(t) \end{bmatrix} \mathbf{p}_i^*, i \in \{1,2,3\} = \mathcal{I}_L \\ \mathbf{p}_1^* &= [2,0]^\top, \mathbf{p}_2^* = [1,1]^\top, \mathbf{p}_3^* = [1,-1]^\top, \mathbf{p}_4^* = [0,1]^\top \\ \mathbf{p}_5^* &= [0,-1]^\top, \mathbf{p}_6^* = [-1,1]^\top, \mathbf{p}_7^* = [-1,-1]^\top \end{aligned} \tag{26}$$

which can be verified to comply with Assumption 1 for arbitrary m with $B = 3$. As a first example in ideal conditions with $\varepsilon = 0$, we set $m = 5$ as well as $\kappa_0 = \cdots = \kappa_5 = 50$ for which it can be verified that

$$\kappa_m = \kappa_5 > B\sqrt{d \cdot N_F \sigma_{\max}(\boldsymbol{\Omega}_{FF}) / \sigma_{\min}(\boldsymbol{\Omega}_{FF})} \approx 46.96$$

such that the design conditions in Theorem 1 are complied. This example with such high-order dynamics can be particularly relevant in the context of quadrotor control, where higher-order derivatives of position are used as inputs when generating trajectories [47].

In all subsequent experiments, discrete-time simulations are carried out using (21), which, as discussed in Section 5.2, is the proper discretization of the main algorithm in (5). In contrast, the follower dynamics (3) are simulated with a forward Euler scheme using a small step size $\Delta_{\text{euler}} = 10^{-5}$ s to accurately approximate the continuous-time behavior. Such step size may differ from the observer step $\Delta > 0$ which represents the time between communication rounds. As a first experiment, we consider a very small observer step $\Delta = 10^{-5}$ s and noiseless leader measurements to approximate the behavior of the ideal continuous-time algorithm (5) and to visualize its performance. In this case the output trajectories of the observer are shown in Figure 1. It can be observed that finite-time convergence to the exact values of the references and its derivatives is achieved before $t \approx 2$ s. Each follower agent is assumed to have integrator dynamics with $m_i = 5$. We used the output of (5) in the local controller (9) for each agent with $\rho_{i,\mu}$ chosen from the coefficients of the polynomial with poles all at -0.1. Some captures for this experiment are shown in Figure 2 where it is observed that the followers' positions converge to the formation dictated by the current positions of the leaders.

Now, we test our observer under noisy measurements and discrete time sampling and compare its performance with other methods in the literature. For comparison, we selected the linear methods described in [10] and the sliding mode method in [15], summarizing the most common approaches to solve the affine formation tracking problem.

To test the proposal's performance under noisy leader measurements, we considered the setting described in Section 5.1 for which we keep $\Delta = 10^{-5}$ s and vary $\varepsilon > 0$. To compare with [10], we selected $m = 1$ in our proposal. Note that the method in [15] cannot be used since it only handles $m = 0$. For the sake of fairness and to test the linear protocol in its ideal setting, we use it as an observer to estimate the components of the target follower positions $-\boldsymbol{\Omega}_{FF}^{-1} \boldsymbol{\Omega}_{LF}^\top \mathbf{p}_L(t)$ and velocities $-\boldsymbol{\Omega}_{FF}^{-1} \boldsymbol{\Omega}_{LF}^\top \dot{\mathbf{p}}_L(t)$.

Figure 3 shows the error trajectories for the position estimation without noise and with noise of magnitude $\varepsilon = 0.2$. The method in [10] was configured with acceleration cancellation and gains such that the settling time is similar to our proposal (see the left side of Figure 3). However, note that our method, being of finite time, can achieve faster convergence with smaller gains. As a result, such selection of gains for the linear method leads to more considerable noise sensitivity, where our method performs consistently better.

Another significant advantage is shown in Figure 4. Here, we compare the estimation error for the velocity over 100 different noise levels $\varepsilon \in [0,2]$. It is observed that while the linear method has better performance under small noise levels, HOSM outperforms it when the noise level increases. The reason is that the maximum error for the linear method grows linearly. In contrast, for HOSM, the error grows as $\varepsilon^{\frac{m-\mu+1}{m+1}} = \sqrt{\varepsilon}$ with $\mu = 1$ as a result of Corollary 1 or more clearly as in Proposition 2 given the small size of the time step Δ, leading to smaller asymptotical error when compared to the linear case.

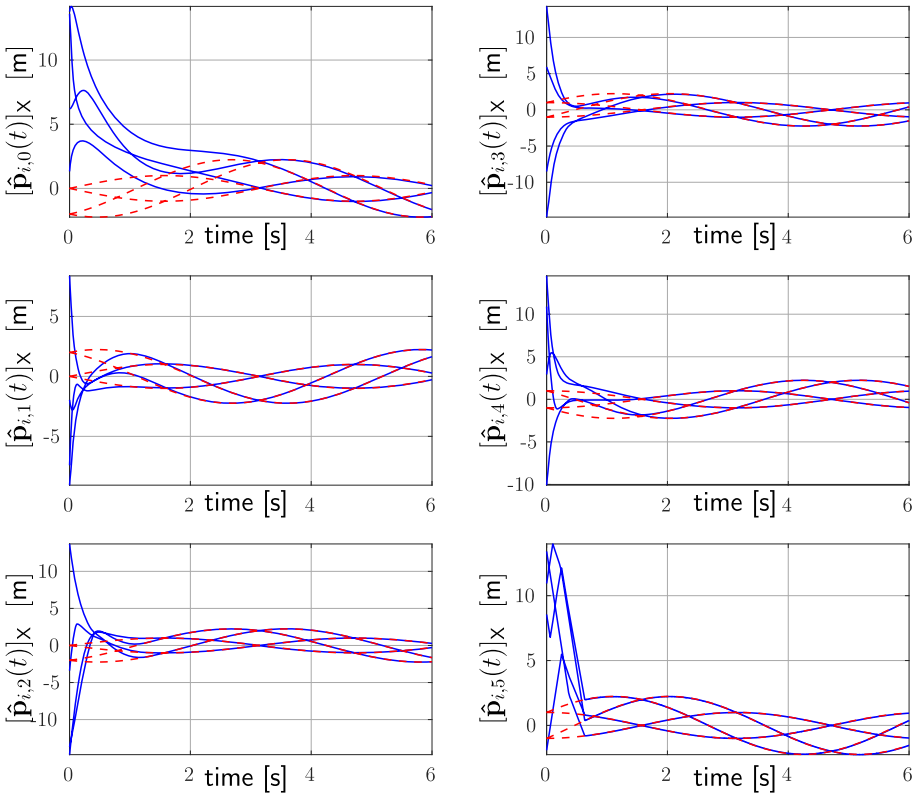

FIGURE 1 | Example trajectories for the X component of $\hat{\mathbf{p}}_{i,\mu}(t)$ for followers $i \in \{4,5,6,7\} = \mathcal{I}_F$ (blue lines) and $m = 5$. Recall that the observer (5) achieves its goal if $\hat{\mathbf{p}}_{i,\mu}(t)$ manages to estimate the components of $-\boldsymbol{\Omega}_{FF}^{-1}\boldsymbol{\Omega}_{LF}^{\top}\mathbf{p}_L^{(\mu)}(t)$ corresponding to the i-th agent. Hence, we show such reference trajectories as well (red dashed lines).

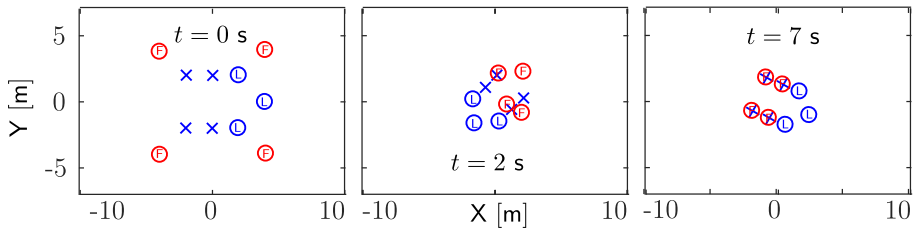

FIGURE 2 | Different frame captures for the trajectories of the agents (see Section 6). Blue (red) circles are leader (follower) positions. Blue crosses are the positions of the followers in the target configuration. The blue circles and crosses define an affine transformation of the nominal configuration. This transformation is a scaling by a factor of two at $t = 0$, and evolves over time according to the trajectories of (26). A video for this experiment can be found in https://rodrigoaldana.github.io/utils/affinevideo.html.

Finally, we show the advantages of our proposal in the discrete-time case, particularly when compared to the FOSM method from [15], which corresponds to (5) with $m = 0$. We performed the same simulation with different values of time step Δ with fixed $\epsilon = 0$. In this case, the errors are caused by the effect of chattering due to the discrete-time switching in the sliding mode. The result is shown in Figure 5, where it is observed that the error for the position variable ($\mu = 0$) is consistently decreased by increasing the protocol order m. This is expected since Proposition 3 ensures worst-case errors proportional to $\Delta^{m-\mu+1}$, which decrease as m is increased for $\Delta < 1$. As a result, our method outperforms that in [15] when $m > 0$. Note that although the simulation step $\Delta_{\text{euler}} = 10^{-5}$ s for the continuous-time system (3) is chosen sufficiently small to accurately capture the plant dynamics, the observer operates with a step size of up to 2×10^{-3} s. This value is on the order of standard communication intervals in digital protocols such as WiFi or Bluetooth. Therefore, the effectiveness of the proposed approach is demonstrated under conditions that are consistent with practical applications.

7 | Conclusions

We presented a hierarchical approach for affine formation tracking relying on a homogeneous communication-based observer. The aim of this observer is to compute the local references for each agent according to an affine transformation of the formation derived from the current position of the leaders. The main novelty of this work relied on the utilization of arbitrary order

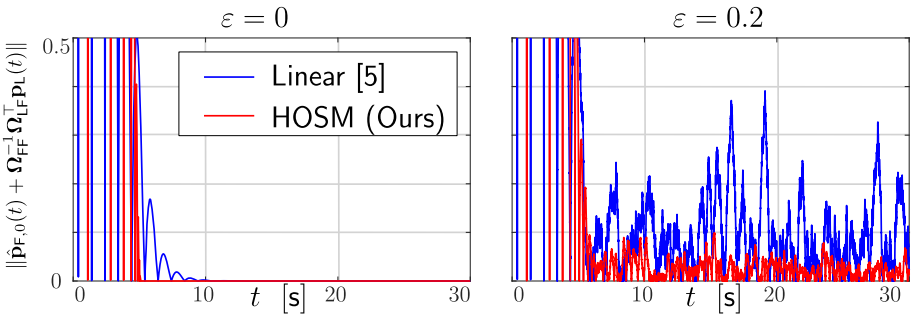

FIGURE 3 | Error trajectories of the proposed observer for position $\|\hat{\mathbf{p}}_{F,0}(t) - (-\mathbf{\Omega}_{FF}^{-1}\mathbf{\Omega}_{LF}^{\top}\mathbf{p}_L(t))\|$ without noise $\varepsilon = 0$ and with noise of maximum bound $\varepsilon = 0.2$. The linear method in [10] with $m = 1$ is compared to our proposal (HOSM).

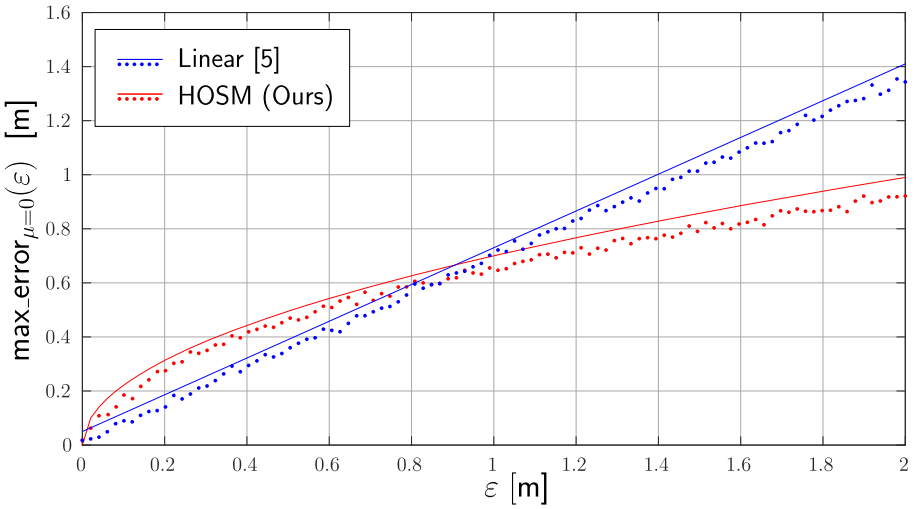

FIGURE 4 | Average steady-state absolute error for the X coordinate of $\hat{\mathbf{p}}_{i,1}(t)$ (velocity $\mu = 1$) under measurement noise for the leader positions for different values of the noise magnitude ε. The linear method in [10] with $m = 1$ is compared to our proposal (HOSM). Solid curves represent worst-case bounds fitted to the experimental data. Linear growth is shown for the linear protocols and of the form $\gamma\sqrt{\varepsilon}$ for HOSM.

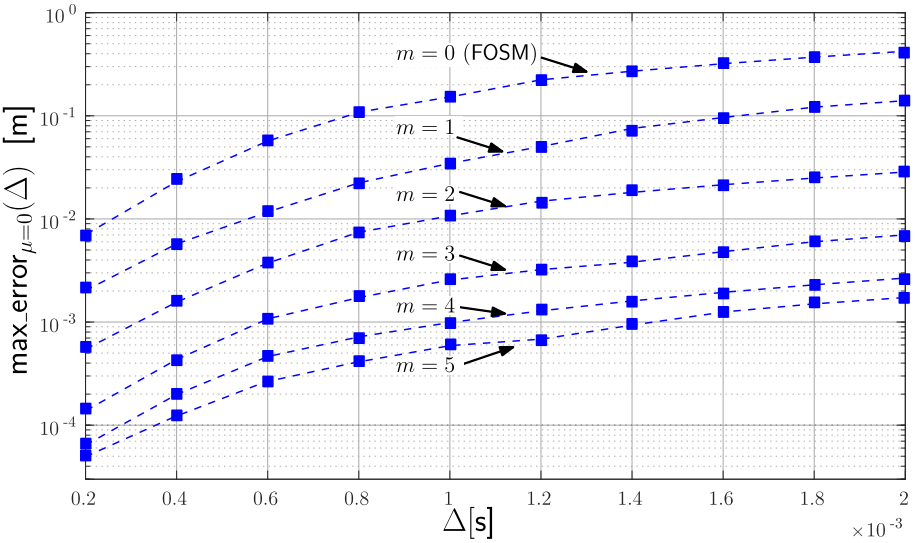

FIGURE 5 | Average steady-state absolute error for the X coordinate of $\hat{\mathbf{p}}_{i,0}[k]$ in (21) for different values of the sampling step Δ and different protocol orders m. Note that the case with $m = 0$ (FOSM) coincides with the method in [15].

homogeneous sliding modes for the observer design, a concept that had not been explored in the literature on affine formations before. We formally demonstrated the exact convergence of the observer in finite time in the ideal case. We provided robustness guarantees against discrete-time communication and measurement noise affecting the leaders' positions. A separation principle for the observer-controller pair was discussed, enabling the use of different controllers or dynamics at each agent. For future work, we consider other scenarios that could involve controlling the motions of the formation leaders, thus expanding the scope of our research.

Acknowledgments

This work was supported via project REMAIN S1/1.1/E0111 (Interreg Sudoe Programme, ERDF), projects PID2021-124137OB-I00 and PID2024-159279OB-I00 funded by MCIN/AEI/10.13039/501100011033, by ERDF A way of making Europe and by the European Union NextGenerationEU/PRTR, by the Gobierno de Aragón under Project DGA T45-23R, by the Universidad de Zaragoza and Banco Santander, and by the Consejo Nacional de Ciencia y Tecnología (CONACYT-Mexico) with grant number 739841.

Conflicts of Interest

The authors declare no conflicts of interest.

Data Availability Statement

The authors have nothing to report.

References

1. K. K. Oh, M. C. Park, and H. S. Ahn, "A Survey of Multi-Agent Formation Control," *Automatica* 53 (2015): 424–440, https://doi.org/10.1016/j.automatica.2014.10.022.

2. G. L pez-Nicol s, M. Aranda, and Y. Mezouar, "Adaptive Multirobot Formation Planning to Enclose and Track a Target With Motion and Visibility Constraints," *IEEE Transactions on Robotics* 36, no. 1 (2020): 142–156, https://doi.org/10.1109/TRO.2019.2943059.

3. M. H. Trinh, S. Zhao, Z. Sun, D. Zelazo, B. D. O. Anderson, and H. S. Ahn, "Bearing-Based Formation Control of a Group of Agents With Leader-First Follower Structure," *IEEE Transactions on Automatic Control* 64, no. 2 (2019): 598–613, https://doi.org/10.1109/TAC.2018.2836022.

4. J. Alonso-Mora, S. Baker, and D. Rus, "Multi-Robot Formation Control and Object Transport in Dynamic Environments via Constrained Optimization," *International Journal of Robotics Research* 36, no. 9 (2017): 1000–1021.

5. L. Krick, M. E. Broucke, and B. A. Francis, "Stabilisation of Infinitesimally Rigid Formations of Multi-Robot Networks," *International Journal of Control* 82, no. 3 (2009): 423–439, https://doi.org/10.1080/00207170802108441.

6. Y. Cao, W. Ren, and Z. Meng, "Decentralized Finite-Time Sliding Mode Estimators and Their Applications in Decentralized Finite-Time Formation Tracking," *Systems & Control Letters* 59, no. 9 (2010): 522–529.

7. Z. Lin, L. Wang, Z. Han, and M. Fu, "Distributed Formation Control of Multi-Agent Systems Using Complex Laplacian," *IEEE Transactions on Automatic Control* 59, no. 7 (2014): 1765–1777.

8. X. Fang, L. Xie, and X. Li, "Distributed Localization in Dynamic Networks via Complex Laplacian," *Automatica* 151 (2023): 110915.

9. Z. Lin, L. Wang, Z. Chen, M. Fu, and Z. Han, "Necessary and Sufficient Graphical Conditions for Affine Formation Control," *IEEE Transactions on Automatic Control* 61, no. 10 (2016): 2877–2891, https://doi.org/10.1109/TAC.2015.2504265.

10. S. Zhao, "Affine Formation Maneuver Control of Multiagent Systems," *IEEE Transactions on Automatic Control* 63, no. 12 (2018): 4140–4155.

11. L. Chen, J. Mei, C. Li, and G. Ma, "Distributed Leader Follower Affine Formation Maneuver Control for High-Order Multiagent Systems," *IEEE Transactions on Automatic Control* 65, no. 11 (2020): 4941–4948, https://doi.org/10.1109/TAC.2020.2986684.

12. Y. Xu, D. Li, D. Luo, Y. You, and H. Duan, "Two-Layer Distributed Hybrid Affine Formation Control of Networked Euler Lagrange Systems," *Journal of the Franklin Institute* 356, no. 4 (2019): 2172–2197.

13. Q. Yang, H. Fang, M. Cao, and J. Chen, "Planar Affine Formation Stabilization via Parameter Estimations," *IEEE Transactions on Cybernetics* 52, no. 6 (2022): 5322–5332, https://doi.org/10.1109/TCYB.2020.3030270.

14. D. Li, G. Ma, Y. Xu, W. He, and S. S. Ge, "Layered Affine Formation Control of Networked Uncertain Systems: A Fully Distributed Approach Over Directed Graphs," *IEEE Transactions on Cybernetics* 51, no. 12 (2021): 6119–6130, https://doi.org/10.1109/TCYB.2020.2965657.

15. Y. Lin, Z. Lin, Z. Sun, and B. D. O. Anderson, "A Unified Approach for Finite-Time Global Stabilization of Affine, Rigid, and Translational Formation," *IEEE Transactions on Automatic Control* 67, no. 4 (2022): 1869–1881, https://doi.org/10.1109/TAC.2021.3084247.

16. Y. Xu, D. Luo, D. Li, Y. You, and H. Duan, "Affine Formation Control for Heterogeneous Multi-Agent Systems With Directed Interaction Networks," *Neurocomputing* 330 (2019): 104–115.

17. J. Wang, X. Ding, C. Wang, L. Liang, and H. Hu, "Affine Formation Control for Multi-Agent Systems With Prescribed Convergence Time," *Journal of the Franklin Institute* 358, no. 14 (2021): 7055–7072.

18. Z. Xu, T. Yan, S. X. Yang, and S. A. Gadsden, "Distributed Leader Follower Formation Control of Mobile Robots Based on Bioinspired Neural Dynamics and Adaptive Sliding Innovation Filter," *IEEE Transactions on Industrial Informatics* 20, no. 2 (2024): 1180–1189.

19. L. Tian, Y. Hua, X. Dong, J. Lü, and Z. Ren, "Distributed Time-Varying Group Formation Tracking for Multiagent Systems With Switching Interaction Topologies via Adaptive Control Protocols," *IEEE Transactions on Industrial Informatics* 18, no. 12 (2022): 8422–8433.

20. R. Aldana-L pez, D. G mez-Guti rrez, R. Arag s, and C. Sag s, "Dynamic Consensus With Prescribed Convergence Time for Multileader Formation Tracking," *IEEE Control Systems Letters* 6 (2022): 3014–3019, https://doi.org/10.1109/LCSYS.2022.3181784.

21. Z. Miao, H. Zhong, Y. Wang, H. Zhang, H. Tan, and R. Fierro, "Low-Complexity Leader-Following Formation Control of Mobile Robots Using Only FOV-Constrained Visual Feedback," *IEEE Transactions on Industrial Informatics* 18, no. 7 (2022): 4665–4673.

22. Y. Xu, S. Zhao, D. Luo, and Y. You, "Affine Formation Maneuver Control of High-Order Multi-Agent Systems Over Directed Networks," *Automatica* 118 (2020): 109004.

23. K. Gao, Y. Liu, Y. Zhou, Y. Zhao, and P. Huang, "Practical Fixed-Time Affine Formation for Multi-Agent Systems With Time-Based Generators," *IEEE Transactions on Circuits and Systems II: Express Briefs* 69, no. 11 (2022): 4433–4437, https://doi.org/10.1109/TCSII.2022.3186395.

24. B. Zhou, B. Huang, Y. Su, W. Wang, and E. Zhang, "Two-Layer Leader-Follower Optimal Affine Formation Maneuver Control for Networked Unmanned Surface Vessels With Input Saturations," *International Journal of Robust and Nonlinear Control* 34, no. 5 (2024): 3631–3655, https://doi.org/10.1002/rnc.7121.

25. P. Su, Z. Shi, J. Yu, X. Dong, Z. Ren, and D. Wang, "Distributed Time-Varying Optimization-Based Protocols for Affine Formation Maneuver," *IEEE Transactions on Industrial Electronics* 72, no. 8 (2025): 8503–8511, https://doi.org/10.1109/TIE.2025.3528506.

26. X. Zhang, Q. Yang, F. Xiao, H. Fang, and J. Chen, "Linear Formation Control of Multi-Agent Systems," *Automatica* 171 (2025): 111935.

27. Q. Yang, M. Cao, H. Garcia de Marina, H. Fang, and J. Chen, "Distributed Formation Tracking Using Local Coordinate Systems," *Systems & Control Letters* 111 (2018): 70–78.

28. P. Yang, R. A. Freeman, and K. M. Lynch, "Multi-Agent Coordination by Decentralized Estimation and Control," *IEEE Transactions on Automatic Control* 53, no. 11 (2008): 2480–2496, https://doi.org/10.1109/TAC.2008.2006925.

29. C. J. Stamouli, C. P. Bechlioulis, and K. J. Kyriakopoulos, "Multi-Agent Formation Control Based on Distributed Estimation With Prescribed Performance," *IEEE Robotics and Automation Letters* 5, no. 2 (2020): 2929–2934, https://doi.org/10.1109/LRA.2020.2970574.

30. D. Li, S. S. Ge, W. He, G. Ma, and L. Xie, "Multilayer Formation Control of Multi-Agent Systems," *Automatica* 109 (2019): 108558.

31. G. Antonelli, F. Arrichiello, F. Caccavale, and A. Marino, "Decentralized Time-Varying Formation Control for Multi-Robot Systems," *International Journal of Robotics Research* 33, no. 7 (2014): 1029–1043.

32. M. Yao, K. Guo, Y. Lu, W. Zhang, and L. Qiao, "Distributed Adaptive Integral Sliding Mode Affine Formation Maneuver Control for Multiple AUVs With Event-Triggered Chattering- Reduction Mechanism," *IEEE Transactions on Vehicular Technology* 73, no. 11 (2024): 16341–16350, https://doi.org/10.1109/TVT.2024.3423771.

33. M. Yao, L. Yu, K. Guo, Y. Lu, W. Zhang, and L. Qiao, "Distributed Two-Layered Leader Follower Affine Formation Control for Multiple AUVs in 3-D Space," *IEEE Transactions on Systems, Man, and Cybernetics: Systems* 55, no. 1 (2025): 85–95, https://doi.org/10.1109/TSMC.2024.3431295.

34. A. Levant, "Higher-Order Sliding Modes, Differentiation and Output-Feedback Control," *International Journal of Control* 76 (2003): 924–941.

35. A. Levant, "Homogeneity Approach to High-Order Sliding Mode Design," *Automatica* 41, no. 5 (2005): 823–830.

36. R. Aldana-Lpez, R. Arags, and C. Sags, "EDCHO: High Order Exact Dynamic Consensus," *Automatica* 131 (2021): 109750, https://doi.org/10.1016/j.automatica.2021.109750.

37. R. Aldana-L pez, R. Arag s, and C. Sag s, "REDCHO: Robust Exact Dynamic Consensus of High Order," *Automatica* 141 (2022): 110320, https://doi.org/10.1016/j.automatica.2022.110320.

38. S. S. Kia, B. Van Scoy, J. Cortes, R. A. Freeman, K. M. Lynch, and S. Martinez, "Tutorial on Dynamic Average Consensus: The Problem, Its Applications, and the Algorithms," *IEEE Control Systems Magazine* 39, no. 3 (2019): 40–72, https://doi.org/10.1109/MCS.2019.2900783.

39. H. K. Khalil, *Nonlinear Systems* (Pearson Education, 2002).

40. G. Hardy, J. Littlewood, and G. Pólya, *Inequalities. Cambridge Mathematical Library* (Cambridge University Press, 1988).

41. F. Arscott and A. Filippov, *Differential Equations With Discontinuous Righthand Sides: Control Systems. Mathematics and Its Applications* (Springer Netherlands, 1988).

42. F. N. Martins, W. C. Celeste, R. Carelli, M. Sarcinelli-Filho, and T. F. Bastos-Filho, "An Adaptive Dynamic Controller for Autonomous Mobile Robot Trajectory Tracking," *Control Engineering Practice* 16, no. 11 (2008): 1354–1363.

43. C. Aguilar-Ib ez, H. Sira-Ram rez, M. S. Su rez-Casta n, E. Mart nez-Navarro, and M. A. Moreno-Armendariz, "The Trajectory Tracking Problem for an Unmanned Four-Rotor System: Flatness-Based Approach," *International Journal of Control* 85, no. 1 (2012): 69–77.

44. M. Lu, L. Liu, and G. Feng, "Adaptive Tracking Control of Uncertain Euler Lagrange Systems Subject to External Disturbances," *Automatica* 104 (2019): 207–219.

45. X. Fang, X. Li, and L. Xie, "3-D Distributed Localization With Mixed Local Relative Measurements," *IEEE Transactions on Signal Processing* 68 (2020): 5869–5881, https://doi.org/10.1109/TSP.2020.3029399.

46. M. Livne and A. Levant, "Proper Discretization of Homogeneous Differentiators," *Automatica* 50, no. 8 (2014): 2007–2014.

47. D. Mellinger and V. Kumar, "Minimum Snap Trajectory Generation and Control for Quadrotors," in *Proceedings of the 2011 IEEE International Conference on Robotics and Automation* (IEEE, 2011), 2520–2525.